Molecular determinants for differential membrane trafficking of PMCA1 and PMCA2 in mammalian hair cells

M'hamed Grati[1,*], Nisha Aggarwal[1], Emanuel E. Strehler[2] and Robert J. Wenthold[1,‡]

[1]Laboratory of Neurochemistry, National Institute on Deafness and other Communication Disorders, National Institutes of Health, Bethesda, MD 20892, USA
[2]Department of Biochemistry and Molecular Biology, Mayo Clinic College of Medicine, Rochester, MN 55905, USA
*Present address: Genetics of Deafness Laboratory, The Wellcome Trust Sanger Institute, Cambridge, CB10, 1SA, UK
‡Author for correspondence (e-mail: wenthold@nidcd.nih.gov)

Accepted 2 May 2006
Journal of Cell Science 119, 2995-3007 Published by The Company of Biologists 2006
doi:10.1242/jcs.03030

Summary

The plasma membrane Ca^{2+}-ATPase-2 (PMCA2) is expressed in stereocilia of hair cells of the inner ear, whereas PMCA1 is expressed in the basolateral plasma membrane of hair cells. Both extrude excess Ca^{2+} from the cytosol. They are predicted to contain ten membrane-spanning segments, two large cytoplasmic loops as well as cytosolic N- and C-termini. Several isoform variants are generated for both PMCA1 and PMCA2 by alternative splicing, affecting their first cytosolic loop (A-site) and their C-terminal tail. To understand how these isoforms are differentially targeted in hair cells, we investigated their targeting regions and expression in hair cells. Our results show that a Leu-Ile motif in 'b'-tail splice variants promotes PMCA1b and PMCA2b basolateral sorting in hair cells. Moreover, apical targeting of PMCA2 depends on the size of the A-site-spliced insert, suggesting that the conformation of the cytoplasmic loop plays a role in apical targeting.

Supplementary material available online at
http://jcs.biologists.org/cgi/content/full/119/14/2995/DC1

Key words: Alternative splicing, Inner ear explant, Intracellular loop, Leucine-isoleucine signal, Stereocilia

Introduction

The plasma membrane Ca^{2+}-ATPases-1 and -2 (PMCA1 and PMCA2) are the major Ca^{2+} pumps of mammalian sensory hair cells (HCs). PMCA1 is located in the HC basolateral membrane, whereas PMCA2 is localized to the mechanosensory stereocilia at the apical pole of HCs (Dumont et al., 2001) (for a review, see Guerini et al., 2005). Both isoforms play major roles in Ca^{2+} extrusion from HCs to maintain a low cytosolic Ca^{2+} concentration. PMCA2 also contributes to the creation of a high extracellular Ca^{2+} concentration around the hair bundle and maintains the Ca^{2+} concentration of the endolymph (Wood et al., 2004). PMCA2 activity is required for normal hearing (Yamoah et al., 1998), and a mutation (G283S) in the mouse *PMCA2* gene causes recessively inherited deafness (Street et al., 1998). A hypofunctional variant of PMCA2 was found in the heterozygous state associated with increased loss of hearing in human patients carrying homozygous mutation in CDH23 (Schultz et al., 2005). PMCA1 and PMCA2 display several splice variants due to the presence of two alternative splicing sites located in the first cytoplasmic loop (A-splice site) and in the C-terminal tail (C-splice region; Fig. 1) (for a review, see Strehler and Zacharias, 2001).

Hair cells of the inner ear are polarized epithelial cells with distinct apical and basolateral plasma membrane (PM) domains that contain different protein and lipid compositions. The apical pole contains a highly specialized stereociliary hair bundle that includes the mechanotransduction apparatus for auditory signals. The basolateral domain contains the synaptic contacts of both inner and outer HCs and, for outer HCs, it also contains the machinery for HC elongation and contraction (Kalinec et al., 1992). Since the apical and basolateral membranes are separated by junctions that do not allow protein and lipid flow, proteins found in only one domain, such as PMCA1 (basolateral) and PMCA2 (apical), require separate delivery systems. Although little is known about protein targeting in HCs, it has been studied extensively in other polarized epithelial cells.

Polarized protein distribution results from sorting mechanisms operating in the biosynthetic and recycling pathways that recognize specific sorting signals in proteins. Structural features, believed to operate as apical sorting signals include glycosylphophatidylinositol anchors (Lisanti et al., 1989; Ikonen, 2001), N-glycans (Scheiffele et al., 1995), O-glycans (Yeaman et al., 1997; Jacob et al., 2000), and protein sequences in the transmembrane domains (TMs) (Kundu et al., 1996; Lin et al., 1998), cytoplasmic domains (Chuang and Sung, 1998; Rodriguez-Boulan and Gonzalez, 1999; Nelson and Yeaman, 2001; Klapper et al., 2006) or extracytoplasmic loop (Qi et al., 2005). However, basolateral signals are typically formed by short, cytoplasmic peptide sequences (Le Gall et al., 1995; Yeaman et al., 1999; Mostov et al., 2000). Among the best-studied basolateral signals are Tyr-based motifs (consensus motif NPxY or YxxF) as well as Leu-Leu and di-hydrophobic residues (Matter et al., 1992; Aroeti et al., 1993; Hunziker and Fumey, 1994; Simonsen et al., 1997;

Bonifacino and Dell'Angelica, 1999; Rodionov et al., 2000) or a single Leu residue (Deora et al., 2004).

The high sequence homology among the PMCA isoforms raises the interesting question of how they are selectively targeted to separate domains in polarized cells. A recent study showed that alternative splicing plays a major role in the targeting of PMCA2 in Madin-Darby canine kidney type-I (MDCK-1) epithelial cells. Chicka and Strehler showed that the A-splice-site insert regulates its targeting to the apical membrane (Chicka and Strehler, 2003). These authors showed that the size of the insertion at the A-splice site of PMCA2 controls its apical targeting, regardless of the C-terminal cassette; a 45-amino-acid (aa) insert at this site (the w-form) resulted in apical targeting, whereas smaller inserts resulted in basolateral targeting.

In this study we investigated the targeting of PMCA1 and PMCA2 in HCs of the rat inner ear by transfecting GFP constructs of wild-type and mutant PMCA cDNAs into cultures of organs of Corti. We focused on the most divergent areas of the molecules corresponding to the first cytoplasmic loop and the alternatively spliced cassettes of the C-terminal. We find that the A-splice-site insert plays a key role in PMCA apical targeting. In addition, the C-splice-site insert influences their basolateral targeting.

Results

Isolation of rat inner ear PMCA2 cDNA clones

A previous study on the sacculus of the bullfrog showed that the predominant PMCA2 splice form is 2va; however, this form is bullfrog specific and not found in mammals. Even though PMCA2 isoforms that contain the 'w' and 'z' inserts and the b-tail and c-tail were detected, they were only present at low abundance (Dumont et al., 2001). The major PMCA1 isoform in bullfrog is the 1xb variant (Dumont et al., 2001). To identify the forms of PMCA expressed in the mammalian organ of Corti, we carried out reverse transcriptase (RT)-PCR with primers that amplify all A and C splice forms on total RNA isolated from the organ of Corti from rat. Cloning the RT-PCR products relevant to the C-splice site, and sequencing more than 100 recombinant clones, showed only a 543-bp-sized insert corresponding to the a-tail variant of PMCA2 (Fig. 2). Similar experiments for the A-splice site showed two inserts of 627 and 762 bp corresponding to the z-loop- and w-loop-variants (Fig. 2). Gel electrophoresis of the PCR products confirmed the presence of the a-, w- and z-forms and showed the relative abundance of these forms, with the w-form predominating. These results suggest that 2wa and 2za are the major splice forms of PMCA2 present in the organ of Corti from rat. To verify that both of these inserts are present in endogenous PMCA2 from HCs, we used primers to amplify the entire molecule. Thirteen recombinant clones containing full-length PMCA2 cDNA were obtained; of these, 12 were the PMCA2wa form and one was the PMCA2za form (data not shown). Although not detected, we cannot rule out low levels of expression of the other splice

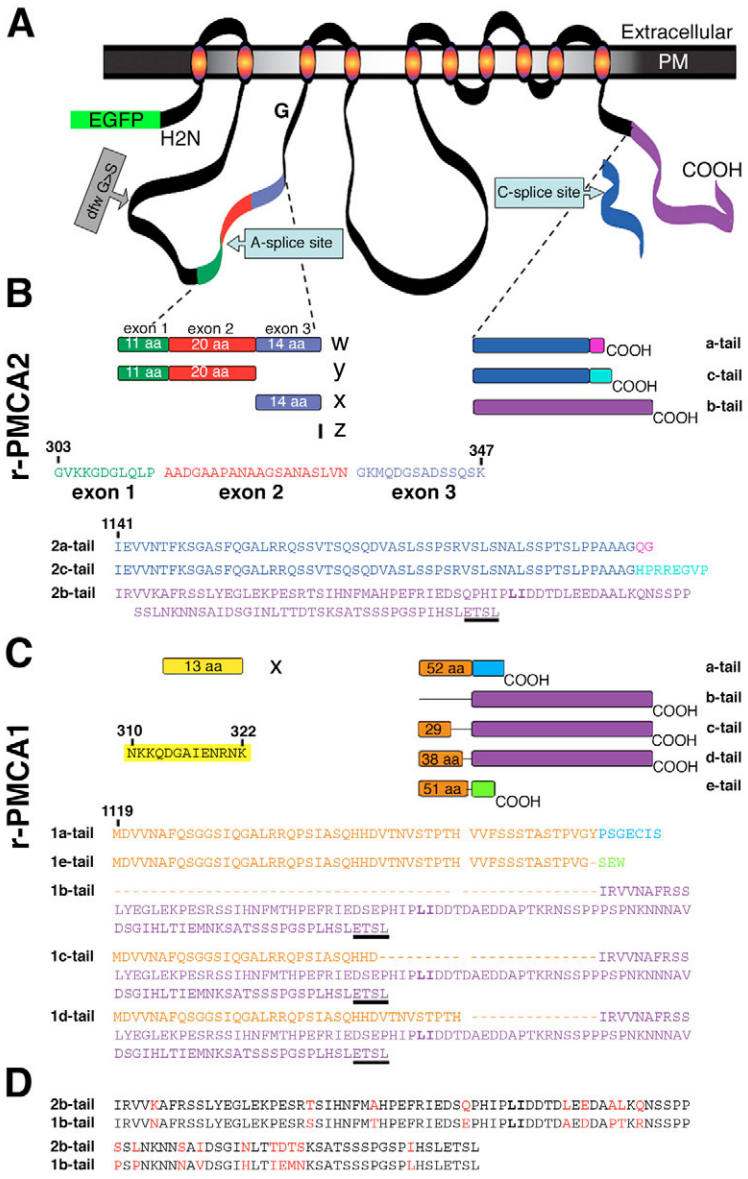

Fig. 1. PMCA1 and PMCA2 alternative splicing. (A) PMCA secondary structure. The positions of the phospholipid binding region (G) and the location of the deafwaddler mouse Gly283Ser mutation (dfw G>S) in PMCA2 are shown. PM, plasma membrane. (B,C) Several PMCA1 and PMCA2 variants are encoded by differentially spliced mRNA. PMCA2 isoforms w, y, x and z are generated by alternative splicing at the A-splice site located in the first cytoplasmic loop. Isoforms differing in their C-termini are generated by alternative splicing at the C-splice site. (B) Aa sequences of PMCA2 exons 1, 2 and 3 of the A-splice site, and of the a-, b- and c-tails generated by alternative splicing at the C-splice site. (C) Aa sequence of the constitutively spliced exon in the PMCA1 A-splice site, and of the a-, b-, c-, d- and e-tails generated by alternative splicing at the C-splice site. Residues Glu-Thr-Ser-Leu (ETSL, underlined in B and C) in the most C-terminal sequence of the b-tail form a PDZ-domain-interacting motif. Aa numbers are according to GenBank PMCA2wb sequence (1243 aa, GenBank accession number P11506), PMCA1xd sequence (1258 aa, GenBank accession number P11505). (D) Aa sequence alignment of PMCA1 and PMCA2 b-tails.

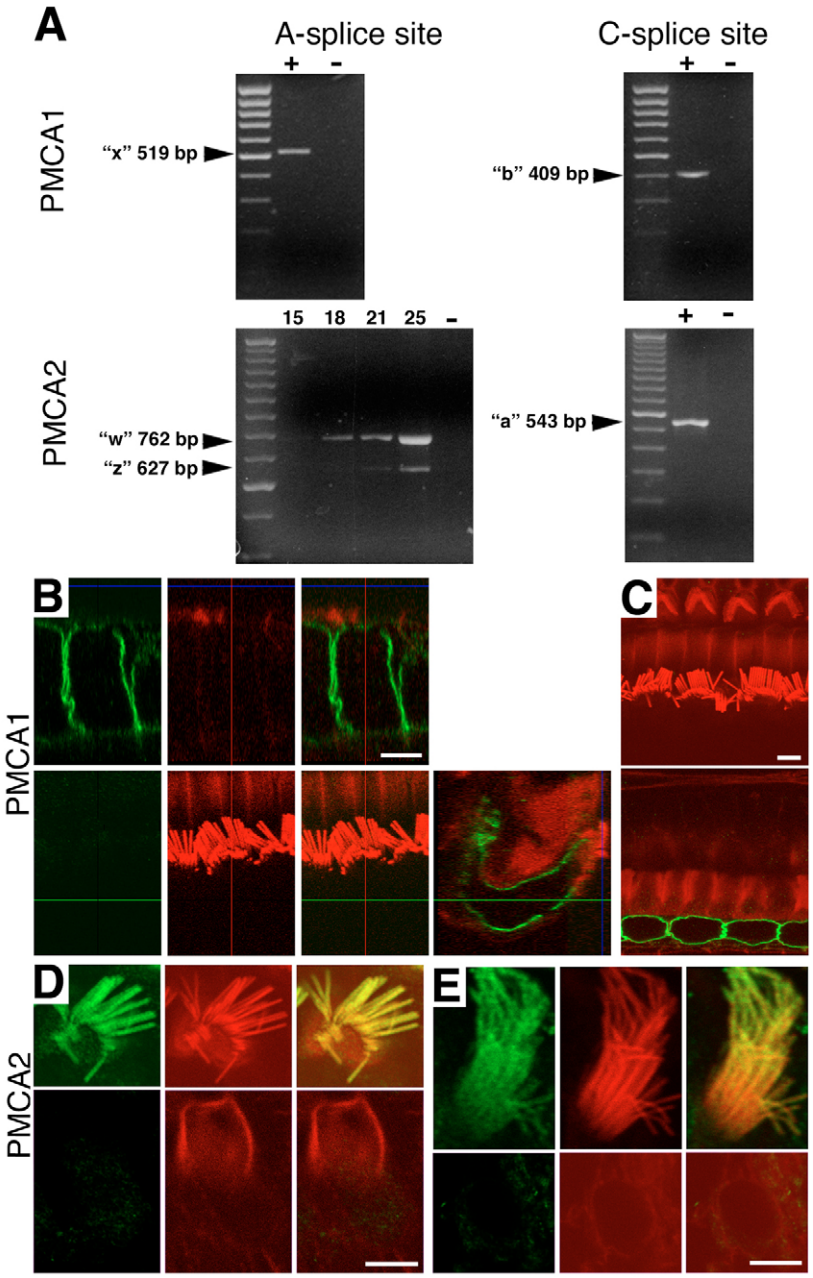

Fig. 2. PMCA1 and PMCA2 in rat inner ear. (A) RT-PCR detection of PMCA1 and PMCA2 isoforms in rat inner ear. Amplification of the A-splice regions of PMCA1 and PMCA2 showed the presence of a unique 519 bp band corresponding to the x-variant (top left), and of two distinct 762 bp and 627 bp bands corresponding to w- and z-variants, respectively (bottom left). RT-PCR product sampling after 15-25 rounds of amplification showed that the w-variant is the dominant form. RT-PCR of the exons encoding the C-terminal tail of PMCA1 and PMCA2 showed the presence of a single 409 bp and 543 bp band, respectively, corresponding to the isoforms encoding the b- and the a-tail, respectively (top right and bottom right, respectively). Thus, only two isoforms of PMCA2, PMCA2wa and PMCA2za, and a single isoform of PMCA1, are detectable in the rat inner ear. +, PCR product after RT; –, PCR product without RT. (B,C) Immunolocalization of PMCA1 in organ of Corti hair cells from rat. Immunofluorescence on adult rat organ of Corti with pan-PMCA1 antibodies reveals abundant labeling in the basolateral PM of inner hair cells. (B) Orthogonal views and stereocilia surface scan of a stack of confocal images are shown in the green (PMCA1), red (actin) and in merged channels. High-resolution hair-bundle surface and transverse basolateral scans in merged channels are also shown in (C). (D,E) Immunolocalization of PMCA2 in rat inner ear hair cells. Immunofluorescence of adult rat inner ear cells with pan-PMCA2 antibodies revealed abundant labeling in the stereocilia (co-stained for actin) of outer HCs (D) and vestibular HCs (E). Hair-bundle surface and transverse basolateral scans are shown in green (PMCA2), red (actin) and merged channels. Bars, 5 μm.

forms, such as those reported by Dumont et al. for the sacculus of the bullfrog (Dumont et al., 2001).

We also carried out RT-PCR on total RNA with primers that would result in amplification of all A- and C-splice forms of PMCA1. For both splice-site RT-PCRs, two single bands of 519 bp and 409 bp, corresponding to the A-splice x-loop variant and to the C-splice b-tail variant, respectively, were isolated, demonstrating that PMCA1xb is the major variant transcribed in the inner ear.

To determine the expression patterns of PMCA1 and PMCA2 in HCs, we used antibodies directed specifically against their respective N-termini to label adult organs of Corti and vestibule explants from rat. Each antibody detects all splice variants of the corresponding PMCA. PMCA1 was exclusively detected in the basolateral PM of inner HCs (Fig. 2) and vestibular HCs (data not shown). It was also localized at low concentration to the basal PM of outer HCs of only the basal turn of the cochlea (data not shown). No traces of PMCA1 were detected in the stereocilia of any type of HCs. PMCA2, however, is consistently found exclusively at the apical PM of outer HCs (Fig. 2), the inner HCs of the apex of the cochlea (data not shown), and vestibular type-I and type-II HCs (Fig. 2). We were unable to detect PMCA2 in the basolateral PMs of vestibular, outer or inner HCs, which indicates that PMCA2 is expressed exclusively in the apical PM of HCs.

Different targeting profiles of PMCA2 isoforms in rat hair cells

In MDCK cells, GFP N-terminally-tagged PMCA2 isoforms were shown to be correctly folded and to behave identically to the non-tagged isoforms (Chicka and Strehler, 2003). We used GFP-tagged PMCA2 constructs in our studies to identify the sorting motifs in its splice variants. We began by examining the A-splice site forms wa and za, which we found to be present in the inner ear based on RT-PCR results.

PMCA2wa contains all three exons in the A-splice site and the a-tail aa sequence in its C-terminus (Fig. 1). It is targeted exclusively to the apical stereociliary hair bundle of HCs (Fig. 3A). Deletion of the a-tail from the PMCA2wa isoform does not alter its exclusive apical targeting (Fig. 3D). However, deletion of all three A-splice-site exons, as found in PMCA2za, leads to a non-polarized distribution to both

basolateral and apical PMs (Fig. 3B). This same non-polarized distribution was seen when we deleted the a-tail for PMCA2za (PMCA2za-del a) (Fig. 3C). This indicates that the presence of the three exons in the first cytosolic loop, as found in PMCA2wa, is crucial for the selective targeting of PMCA2 to the apical PM, whereas the a-tail does not influence targeting.

We next examined the role of the b-tail in PMCA2 targeting by appending the b splice form to PMCA2z, which lacks an apical A-splice site insert. This PMCA2zb isoform is targeted

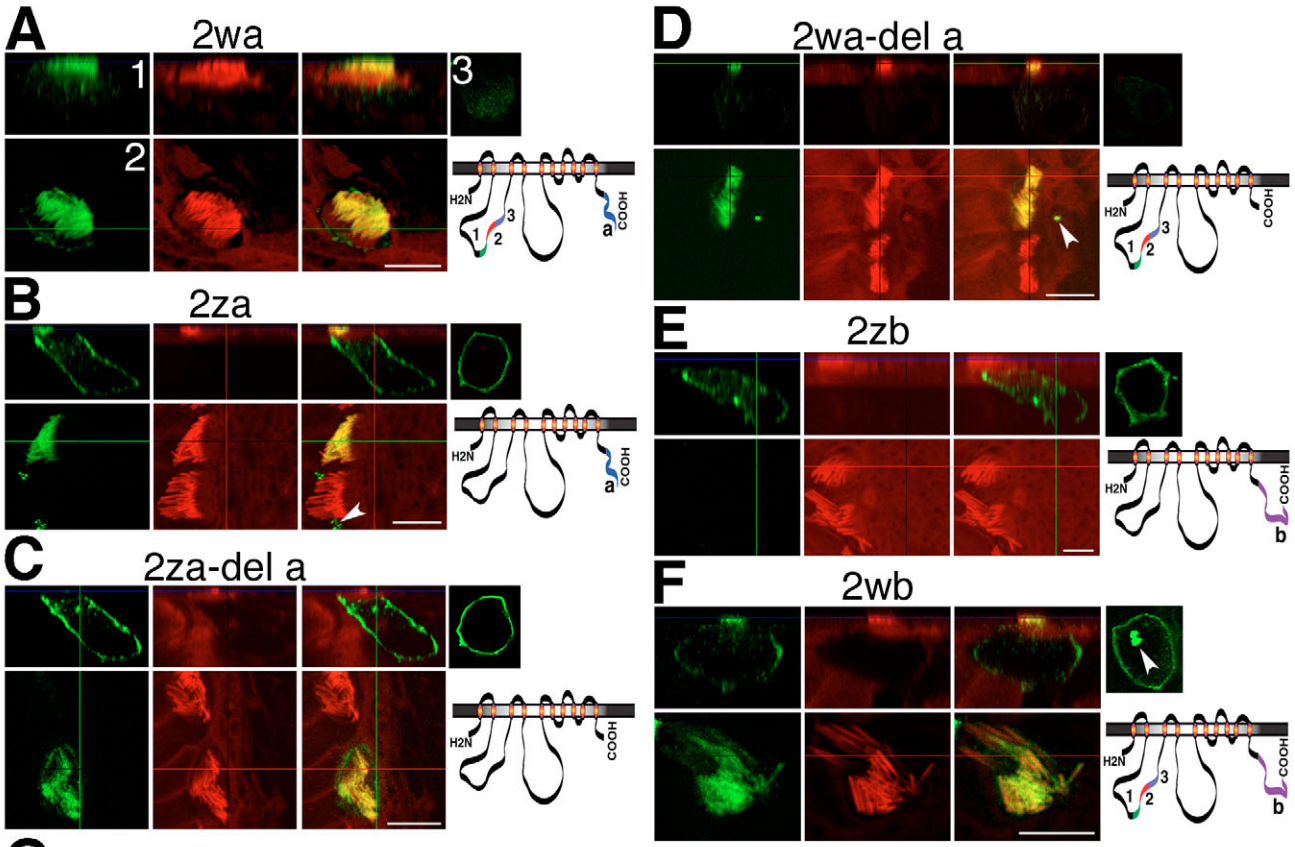

H

Isoform	A splice insert size (aa)	C-splice site content	Polarity	Number of examined HCs	Figure
2wa	45	a	AP	21	3A
2za	0	a	AP+BL	7	3B
2za-del a	0	deleted	AP+BL	4	3C
2wa-del a	45	deleted	AP	4	3D
2zb	0	b	BL	7	3E
2wb	45	b	AP+BL	4	3F

Fig. 3. Alternative A-site and C-site splicing affect apical and basolateral localization of PMCA2 isoforms in HCs. (A-F) Explant HCs were transfected with various EGFP-tagged PCMA2 isoform constructs and examined by immunofluorescence. An apical surface-scan of the stereocilia hair bundle (scanning plane 2 drawn in the HC schematic in G; actin labeled in red) and transverse view of the basolateral plasma membrane (plane 1 drawn in G) of a transfected HC expressing a transgene encoding for each of the EGFP-tagged PMCA2 isoforms (green) are shown in green and red, and merged channels. Arrowheads indicate strong light-scattering signal from the 1-μm-diameter gold bullets collected at 530-550 nm. Bars, 5 μm. Constructs are illustrated on the right. (G) Basolateral cross-sectional scan taken around the midpoint of the transfected HC is also shown on the right of the upper panel (scanning plane 3). (H) Summary of our data. a, a-tail; b, b-tail; AP, apical PM localization; BL, basolateral PM localization.

exclusively basolaterally in HCs (Fig. 3E). This basolateral signal is not dominant over the A-splice-site signal however, because a construct containing both the cytosolic loop exons and the b-tail (PMCA2wb) is delivered to both the apical and basolateral PMs (Fig. 3F). These results suggest that the b-tail contains a signal that results in a vectorial basolateral targeting in the absence of A-splice site inserts. In the presence of A-splice site inserts, targeting is to both poles suggesting a competition between the apical and basolateral signals present in A-splice site inserts and the b-tail, respectively.

We were also interested in studying the targeting properties of PMCA1 in HCs; PMCA1 has over 85% aa sequence homology with PMCA2. The wild-type PMCA1xb, which is the only isoform detected by RT-PCR in the inner ear, is targeted exclusively basolaterally in HCs (Fig. 4B). The b-tail-deleted PMCA1xb variant is targeted to both apical and basolateral PM of HCs (Fig. 4C), suggesting a crucial role of the b-tail for the vectorial basolateral targeting of this pump. This demonstrates that the b-tails of both PMCA1 and PMCA2, which show a high degree of aa homologies (Fig. 1D), encompass the molecular determinant for their targeting. Given the high degree of homology between the two b-tails, we have focused our mutagenesis study on the PMCA2xb-encoding construct to identify the motif(s) necessary for basolateral targeting.

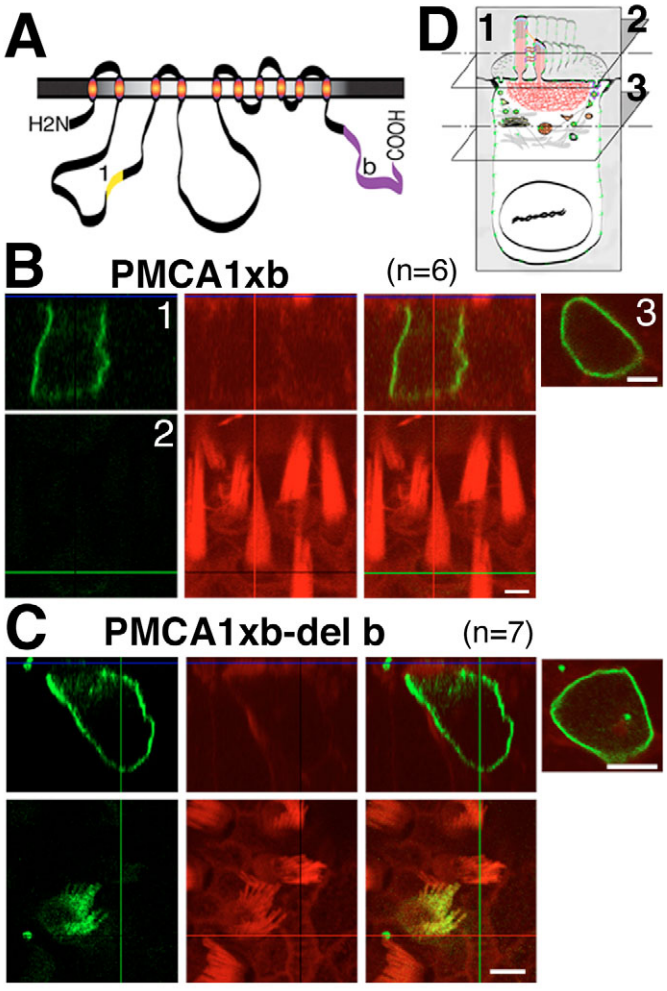

Fig. 4. PMCA1xb basolateral localization in HCs requires the b-tail. (A) Secondary structure of PMC1xb with a single insert (13 aa) in the A-splice site (1, yellow) and the b-tail (b, purple). (B,C) Surface scans (plane 2 in D) and orthogonal views (plane 1 in D) of stacks of confocal images of HCs transfected with wild-type EGFP-tagged PMCA1xb (B) and PMCA1xb deleted of the b-tail aa sequence (C); green (GFP), red (actin), yellow (merged). Small panels show high-resolution cross-sectional (plane 3 drawn in D) scans in merged channels. n, number of examined transfected hair cells. Bars, 5 μm.

A Leu-Ile motif is required for vectorial basolateral targeting of PMCA1 and PMCA2 in HCs

To identify the crucial aa-residues for the basolateral targeting of PMCA2 present in the b-tail (103 aa), we used the isoform PMCA2xb, which traffics identically to PMCA2zb and to PMCA1xb, and is targeted exclusively to the basolateral PM of HCs (Fig. 6B) and MDCK-I cells (supplementary material Movie 1), to perform site directed mutagenesis experiments on the b-tail amino-acid sequence. We studied the role of the potential AP-adaptor-binding tyrosine-based motif YEGL (at positions 1121-1124) and the C-terminal PDZ-domain-interacting motif ETSL (at positions 1209-12), in the basolateral targeting of PMCA2xb. We generated single mutants 2xb-Y1121A and 2xb-del ETSL[1209-12], and the double mutant 2xb-Y1121A-del ETSL and imaged their location in HCs. All three variants were exclusively basolaterally targeted (Fig. 5A-C), showing that these two motifs do not influence the basolateral targeting of PMCA2. We then performed serial deletions in the b-tail of the PMCA2xb isoform. Deletion of the 46 C-terminal aa of the b-tail in PMCA2xb wild type did not alter the targeting of the resulting variant 2xb-del46[1167-ter] in HCs (Fig. 6C). However, the deletion of 65 aa of the C-terminal (1148-ter) of PMCA2xb – variant 2xb-del65[1148-ter] – resulted in the delivery to both apical and basolateral PMs (Fig. 6D). The variant PMCA2za-del a gave similar results (Fig. 3). The deletion of 14 aa at positions 1153-1166 also altered the targeting of PMCA2xb – the variant 2xb-del14[1153-66] (Fig. 6E) – and the variant 2xb-Y1121A-del14-delETSL (Fig. 5D). Thus, these 14 aa are crucial for targeting PMCA2xb exclusively basolaterally. Partial deletion of this region showed that the seven-aa sequence Leu-Ile-Asp-Asp-Thr-Asp-Leu (at positions 1153-1159) was necessary for the exclusively basolateral localization (Fig. 6F). The adjacent downstream sequence Glu-Glu-Asp-Ala-Ala-Leu-Lys did not appear to be important for the targeting of the pump, because the deletion of these residues did not change the exclusively basolateral delivery of PMCA2xb (Fig. 6G). A closer look at aa-sequence alignment of the b-tail of rat and human PMCA1, PMCA2, PMCA3 and PMCA4, showed that three hydrophobic residues, Pro-Leu-Ile at position 1152-1154 in PMCA2xb, are fully conserved among PMCA1, PMCA2 and PMCA3, and are Pro-Leu-Leu in human PMCA4 (Fig. 7C). Leu-Leu or Ile-Leu motifs have been found to act as basolateral targeting motifs in several proteins including E-Cadherin, CD4, GLUT4 and TRP-1 (for a review, see Bonifacino and Traub, 2003). The conserved residues Pro-Leu-Ile (1183-1185) might play identical roles in all PMCAs. Pro1152Ala substitution in wild-type PMCA2xb did not alter the basolateral targeting of the protein (Fig. 7D). However, Leu1153Ala and Ile1154Ala substitutions in wild-type PMCA2xb altered the basolateral

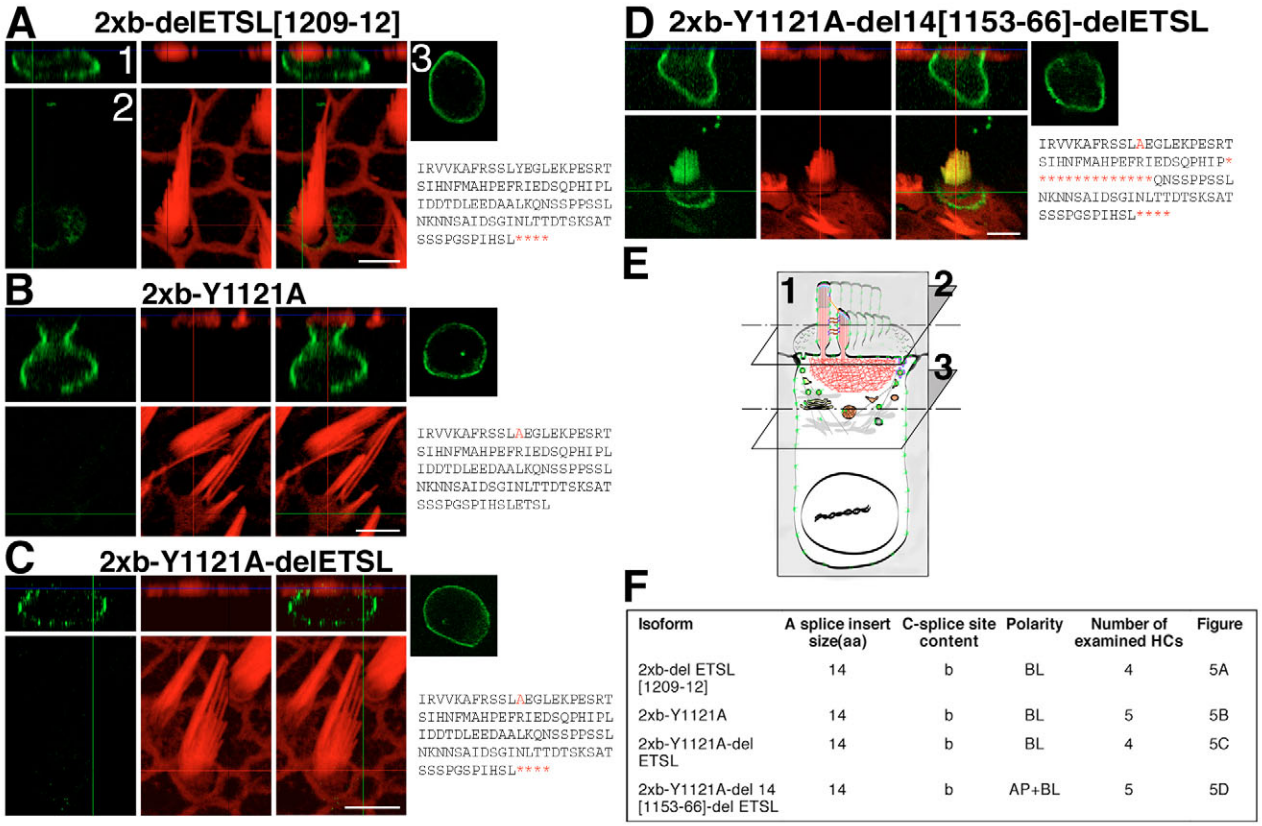

F

Isoform	A splice insert size(aa)	C-splice site content	Polarity	Number of examined HCs	Figure
2xb-del ETSL [1209-12]	14	b	BL	4	5A
2xb-Y1121A	14	b	BL	5	5B
2xb-Y1121A-del ETSL	14	b	BL	4	5C
2xb-Y1121A-del 14 [1153-66]-del ETSL	14	b	AP+BL	5	5D

Fig. 5. The PDZ motif and tyrosine-based motif are not important for PMCA2xb targeting in HCs. (A-D) Surface scans (plane 2 in E) and orthogonal views (plane 1 in E) of stacks of confocal images of HCs transfected with mutated PMCA2xb in separate and merged channels. Small panels on the right show cross-sectional high-resolution scan (plane 3 in E) of the basolateral PM taken around the midpoint of the transfected HC in merged channel. Aa sequences of the b-tail; mutations are in red. The Tyr-based Tyr-Glu-Gly-Leu motif at position 1121-1124 (YEGL), is not a basolateral targeting motif for PMCA2 (B,C). The C-terminal PDZ-domain-interacting Glu-Thr-Ser-Leu motif at position 1209-1212 (ETSL), does not seem to influence the basolateral targeting of the pump (A,C). However, the deletion of residues 1153-1166 in the double mutated Tyr1121Ala isoform and the deletion of the ETSL motif alters the vectorial basolateral targeting of the protein and causes it to localize to the apical pole as well (D). (F) Summary of our data. b, b-tail; AP, apical PM localization; BL, basolateral PM localization. Bars, 5 μm.

targeting of the protein in HCs (Fig. 7E,F). However, the substitution of the downstream acidic aa residues into Ala did not alter the localization of PMCA2xb (Fig. 7H). Moreover, the single substitution of Leu1165Ala, which is similar to the CD147 basolateral targeting motif (see aa alignment in Fig. 7B), did not alter the exclusively basolateral targeting of the pump (Fig. 7G). Combining both substitutions also did not alter the targeting (Fig. 7I). Together, these observations allowed us to conclude that residues Leu1153-Ile1154 are necessary for the targeting of PMCA2xb. These hydrophobic residues are conserved in all mammalian PMCA b-tails (see aa alignment in Fig. 7C) and are likely to be necessary for the localization of these members of the PMCA family.

The b-tail basolateral targeting information is transposable to other transmembrane proteins and is recognized by LLC-PK1 epithelial cells

Different types of epithelial cells vary widely in the final distribution of PM proteins or in the pathways that these proteins follow to the cell surface (Keller and Simons, 1997). In the pig-kidney epithelial (LLC-PK1) cell line, some basolateral membrane proteins exhibit a defect in targeting, resulting in their appearance at the apical surface (Roush et al., 1998; Folsh et al., 1999; Gan et al., 2002). This defect is due to the absence of the μ1B subunit of the adaptin AP1B in these cells (Ohno et al., 1999; Roush et al., 1998; Folsh et al., 1999). We verified the absence of the μ1B subunit by visualizing the apical endocytosis of labelled-transferrin in polarized LLC-PK1 cells (data not shown). Although AP1B has a preference for a consensus Tyr motif through the μ1 subunit (Ohno et al., 1998), it has been shown that the β subunit (Rapoport et al., 1998), and/or γ-σ1 subunit combination (Janvier et al., 2003) of AP1 can bind to Leu-Leu motifs. Alternatively, an accessory protein like PACS-1 might be acting as a piggy-back linker (Rapoport et al., 1998; Wan et al., 1998). Moreover, AP1B has been implicated in targeting cargo in the biosynthetic pathway as well as in the recycling route (Folsh et al., 1999; Gan et al., 2002). In the case of PMCA, transfected LLC-PK1 cells exhibited exclusively basolateral polarity for PMCA2xb (Fig. 8A) and PMCA1xb (data not shown). Thus, the sorting machinery responsible for basolateral sorting of PMCA1xb and PMCA2xb is present in both HCs and LLC-PK1 cells and recognizes LI(1153-54).

To test the transposability of the basolateral targeting information in PMCA1 and PMCA2 b-tails, we transfected

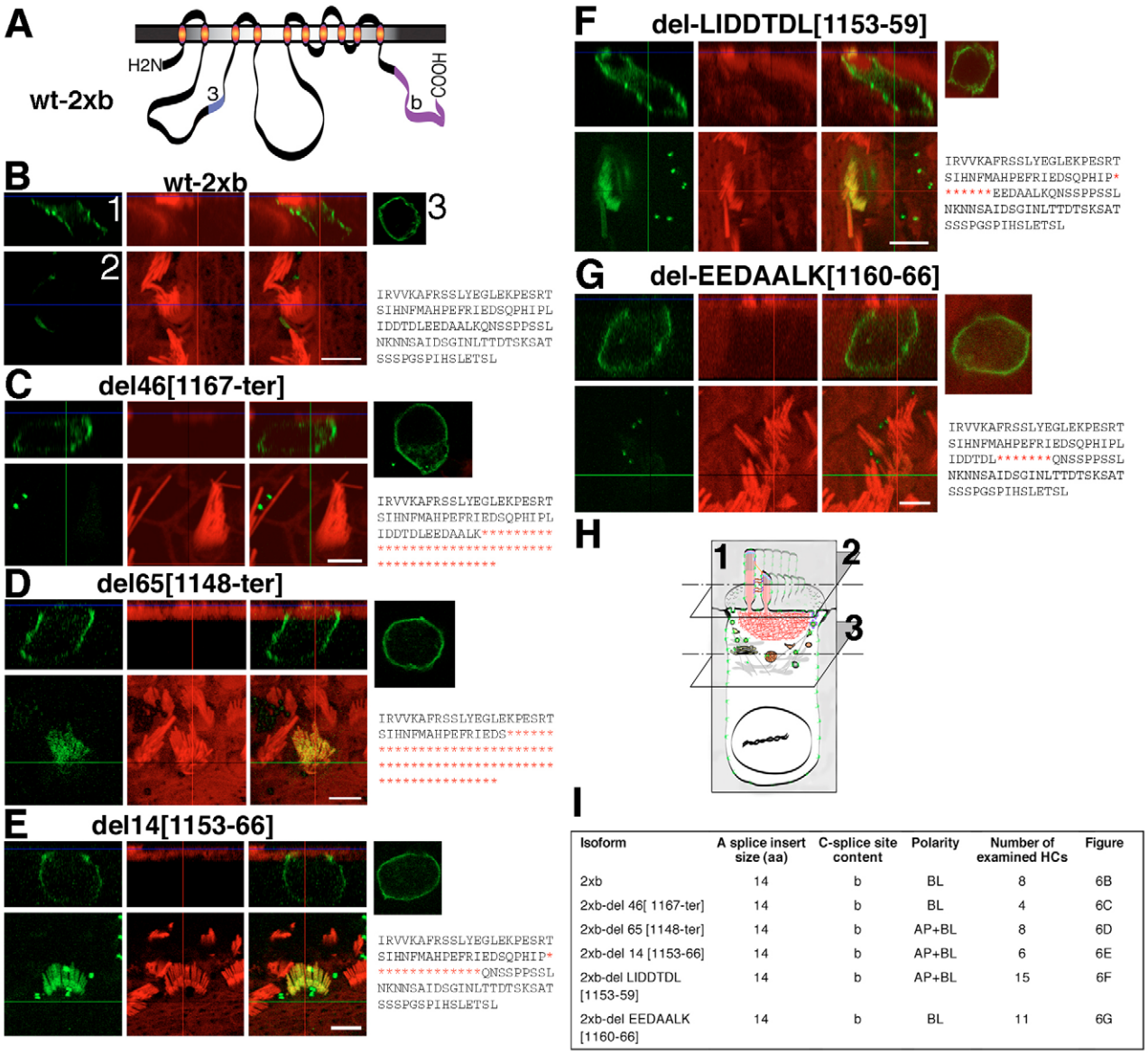

Isoform	A splice insert size (aa)	C-splice site content	Polarity	Number of examined HCs	Figure
2xb	14	b	BL	8	6B
2xb-del 46[1167-ter]	14	b	BL	4	6C
2xb-del 65 [1148-ter]	14	b	AP+BL	8	6D
2xb-del 14 [1153-66]	14	b	AP+BL	6	6E
2xb-del LIDDTDL [1153-59]	14	b	AP+BL	15	6F
2xb-del EEDAALK [1160-66]	14	b	BL	11	6G

Fig. 6. Identification of a region encompassing the basolateral signal in the b-tail. (A) Schematic representation of the wild-type PMCA2xb isoform (wt-2xb) used as a basic isoform for the determination of the basolateral-targeting motif present in the b-tail. (B-G) Apical surface-scan of the hair bundle (plane 2 in H, actin in red) and an orthogonal view of the basolateral plasma membrane (plane 1 in H) of a transfected hair cell expressing a transgene encoding EGFP-tagged (in green) PMCA2xb isoform (wt-2xb) and derived mutated isoforms, are presented in separated green and red, and merged channels. Small panels on the right show high-resolution basolateral cross-sectional scans (plane 3 in H). For each mutated variant, the corresponding mutation is shown in red on the b-tail aa sequence. The aa sequence Leu-Ile-Asp-Asp-Thr-Asp-Leu (LIDDTDL) at position 1153-1159 encompasses the crucial residues for the basolateral targeting of PMCA2xb (F). (I) Summary of our observations. 2xb, wild-type PMCA2xb isoform; b, b-tail; AP, apical PM localization; BL, basolateral PM localization. Bars, 5 μm.

LLC-PK1 cells with constructs encoding the interleukin-2 receptor α-chain (Tac) – which is 200 aa long and has a single C-terminal TM domain (GenBank CAH73597) – and Tac-2b-tail chimera (encoding Tac fused C-terminally to the PMCA2 b-tail aa sequence). Tac was predominantly targeted to the apical PM of LLC-PK1 (Fig. 8B), MDCKI and HCs (data not shown). However, Tac-2b-tail chimera exhibited exclusively basolateral polarity in LLC-PK1 (Fig. 8C). However, the Tac-2b-tail chimera with Leu1153Ala and Ile1154Ala substitutions was predominantly apically targeted in LLC-PK1 (Fig. 8D), similar to the PM localization of Tac alone. These observations support the transposability of the basolateral targeting information encompassed in PMCA1 and PMCA2 b-tails.

Apical targeting of b-tail lacking PMCA2 isoforms is determined by the size of their first cytoplasmic loop

We showed by RT-PCR that PMCA2wa, lacking the b-tail, is the major PMCA2 isoform detected in the inner ear (Fig. 2). This isoform has the A-splice site cassettes that play a dominant role in its exclusive apical targeting in HCs (Fig. 3) and MDCKI cells (supplementary material Movie 2). Thus, we used the cDNA construct encoding this isoform fused to EGFP

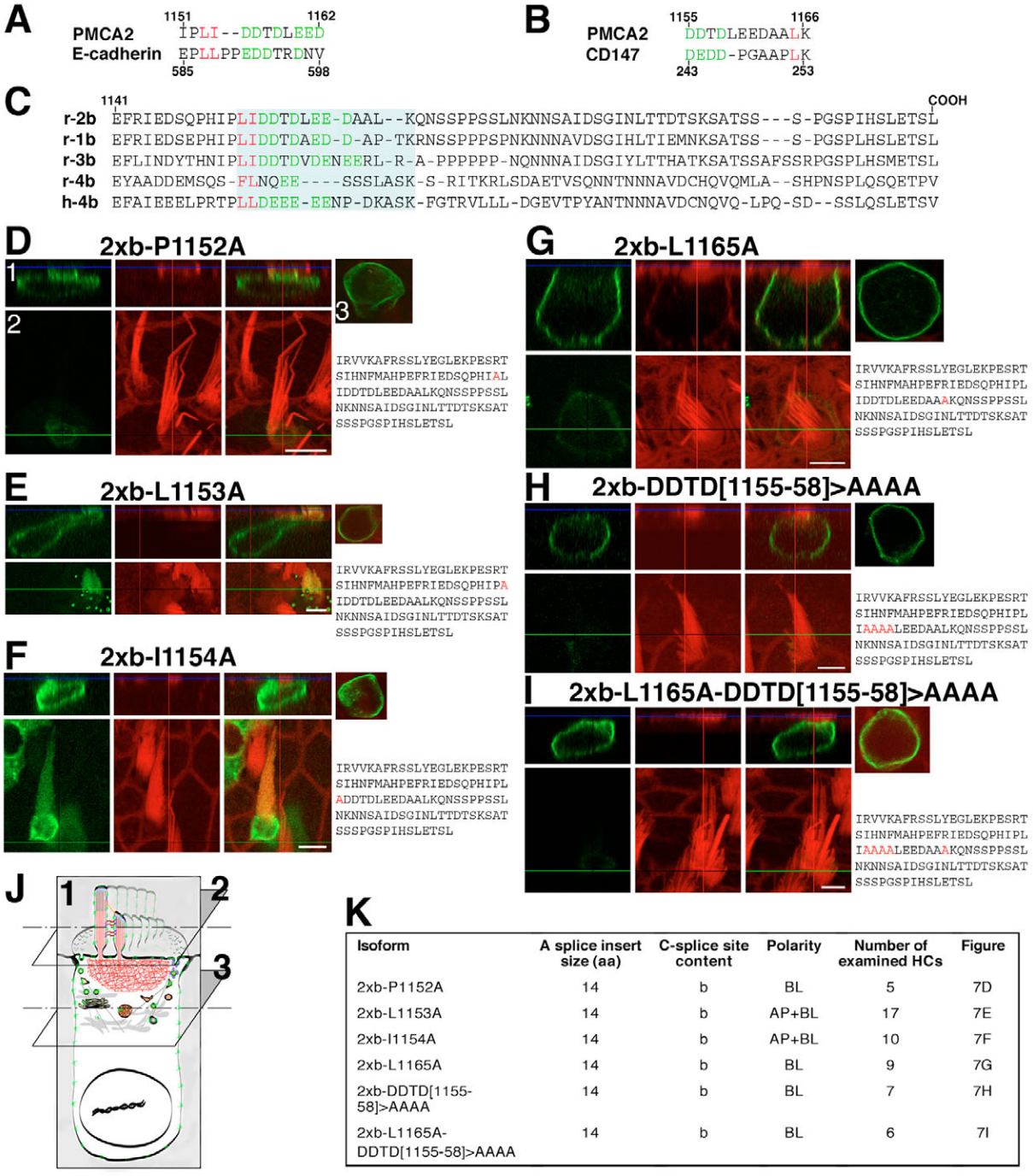

Isoform	A splice insert size (aa)	C-splice site content	Polarity	Number of examined HCs	Figure
2xb-P1152A	14	b	BL	5	7D
2xb-L1153A	14	b	AP+BL	17	7E
2xb-I1154A	14	b	AP+BL	10	7F
2xb-L1165A	14	b	BL	9	7G
2xb-DDTD[1155-58]>AAAA	14	b	BL	7	7H
2xb-L1165A-DDTD[1155-58]>AAAA	14	b	BL	6	7I

Fig. 7. A Leu-Ile motif is required for the basolateral targeting of PMCA2xb. (A,B) Alignment of the basolateral targeting motifs of (A) E-cadherin and (B) CD147 with the crucial aa region for the basolateral targeting of PMCA2. Aa in red indicate the targeting motif of E-cadherin Leu587-[Leu/Ile588] and its homolog in PMCA2 Leu1153-Ile1154 (A), and the crucial residue Leu252 of CD147 and its homolog in PMCA2, Leu1165 (B). Aa in green indicate acidic aa residues. (C) Alignment of the distal C-terminal aa sequences of the b-tail of PMCA1, PMCA2, PMCA3, PMCA 4 from rat and from human PMCA4. Aa in red indicate the Leu[Leu/Ile] motif, aa in green indicate acidic residues, green shading indicates the conserved basolateral targeting motif found in all these PMCAs. Note the conservation of Leu1153-[Leu/Ile1154] and the downstream acidic residues in all four PMCAs. However, Leu1165, which is homologous to the residue crucial for targeting of CD147, is not conserved in all PMCAs. (D-I) Apical surface-scan of the hair bundle (plane 2 in J, actin in red) and an orthogonal view of the basolateral plasma membrane (plane 1 in J) of a transfected hair cell expressing a transgene encoding the EGFP-tagged PMCA2xb isoform (green) (wt-2xb; see Fig. 6A) and derived mutated isoforms, presented in separated green and red, and merged channels. High-resolution basolateral cross-sectional scans (plane 3 in J) are also shown in merged channels. Mutations are shown in red on the aa sequence of the b-tail. Substitutions Leu1153Ala and Ile1154Ala alter the basolateral targeting of PMCA2xb, whereas Phe1152Ala does not. The acidic cluster Asp-Asp-Thr-Asp at position 1155-1158 is not essential for the basolateral targeting of PMCA2xb. (K) Summary of our data. aa, amino acid; b, b-tail; AP, apical PM localization; BL, basolateral PM localization. Bars, 5 μm.

and generated a series of mutations in the alternatively spliced cassettes of the first cytoplasmic loop to identify the crucial determinants for its exclusively apical targeting. Mutations included constructs encoding EGFP-tagged PMCA2ya by deleting exon 3, PMCA2xa by deleting exon 1 and exon 2, PMCA2wa-del(ex1) by deleting exon 1, PMCA2wa-del(ex2) by deleting exon 2 and PMCA2wa-del(ex1-ex3) by deleting exon 1 and exon 3. In HCs, only PMCA2wa, PMCA2ya and PMCA2wa-del(ex1) were targeted exclusively to the apical PM (Fig. 9). The A-splice-insert sizes are 45, 31 and 34 aa for 2wa, 2ya and 2wa-del(ex1), respectively. Isoforms 2za, 2wa-del(ex2) and 2wa-del(ex1-ex3) with insert sizes of 0, 25 and 20 aa, respectively, were targeted to both apical and basolateral poles (Figs 3, 9). All isoforms targeted exclusively to the apical pole contained exon 2, suggesting that exon 2 contains sufficient information for apical targeting. However, the presence of exon 2 alone was insufficient to exclusively target the molecule to the apical pole, because 2wa-del(ex1-ex3) was targeted to the apical and the basolateral pole (Fig. 9). To further investigate the role of exon 2 in targeting, we generated constructs encoding PMCA2wa lacking nine aa in exon 2 [2wa-del(9-ex2)] and PMCA2wa lacking 11 aa in exon 2 [2wa-del(11-ex2)]. We also substituted the sequence of exon 2 in the PMCA2wa isoform with a completely random aa sequence to generate the isoform 2wa-(ex2-sub). All of the generated isoforms were targeted exclusively to the apical PM (Fig. 9), indicating that no specific apical targeting motif is present in exon 2. Rather, our results suggest that the size of the A-splice-site insert is an important factor for apical targeting. None of the constructs eliminated apical targeting completely, indicating that the absence of an A-splice-site insert results in the delivery to both poles – as seen for 2za (Fig. 3) – which might occur by default.

Our results suggest that A-splice-site inserts are not directly responsible for targeting of PMCA2 in HCs but can influence the targeting. Therefore, the targeting signals might reside elsewhere on the first cytoplasmic loop or the bordering TM2 and TM3. Thus, we investigated the role in apical trafficking of two known domains in the first cytoplasmic loop of PMCA2. We generated a 12 aa deletion in the conserved region of the phospholipid-binding site (G-domain), which is located downstream of the A-splice site (Filoteo et al., 1992). The encoded isoform, 2wa-del12(380-91) was targeted exclusively apically (Fig. 10), showing that the targeting of PMCA2 is independent of the G-domain. We also reproduced the Gly283Ser mutation that was detected in the deafwaddler (dfw) mutant mouse and is located upstream of the A-splice site. The 2wa-dfw(G283S)-encoded protein was targeted exclusively apically (Fig. 10), showing that in HCs, this spontaneous mutation does not alter the apical targeting properties of PMCA2.

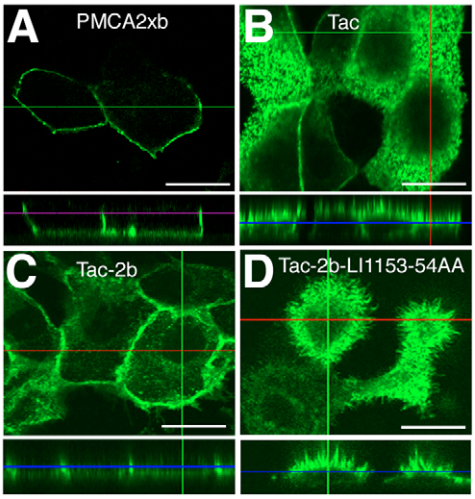

Fig. 8. The basolateral targeting of PMCA2 is not mediated by adaptin AP1B, and the targeting signal is transposable to other PM proteins. (A-C) High-resolution surface confocal scans of transfected polarized LLC-PK1 cells, taken around the junctional area (upper panels) and orthogonal views of stacks of confocal images (lower panels). (A) PMCA2xb (green) is exclusively basolaterally targeted in LLC-PK1. (B) IL-chain (Tac) is delivered predominantly apically in LLC-PK1 cells, with a visible basolateral component. Under the influence of the b-tail, the chimeric protein Tac, fused to the b-tail (Tac-2b), is predominantly delivered to the basolateral PM (C). The mutations in the b-tail Leu1153Ala and Ile1154Ala, inactivate the signal in the b-tail and the product of construct Tac-2b-LI1153-1154AA is targeted predominantly apically (D), similarly to the Tac alone. Bars, 10 μm.

Discussion

To better understand the mechanisms by which proteins are selectively targeted in hair cells of the mammalian inner ear, we investigated the trafficking of two relatively abundant proteins, PMCA1 and PMCA2. These are highly homologous proteins but have very different distribution patterns in hair cells, with PMCA1 confined to the basolateral membrane and PMCA2 to the apical membrane. We focused on the areas of the molecules that are most divergent, the alternatively spliced cassettes of the first intracellular loop and the C-terminus. Using GFP-tagged constructs of PMCA1 and PMCA2 and transfection of hair cells in explant cultures, we show that both sites play roles in determining apical or basolateral destinations.

PMCA1 and PMCA2 isoforms are expressed in rat HCs

A previous study on the sacculus of the bullfrog showed that the predominant PMCA2 splice form is 2va, a form not found in mammals, and the prominent PMCA1 is 1xb (Dumont et al., 2001). Using RT-PCR we found that two isoforms of PMCA2, PMCA2wa and PMCA2za, are the predominant forms expressed in the inner ear of the rat. Our semi-quantitative analysis showed that PMCA2wa is the more abundant isoform. We detected a single form of PMCA1, PMCA1xb. Expression of GFP-tagged constructs of these isoforms reproduced the patterns of distribution obtained with antibodies specifically recognizing PMCA1 and PMCA2. Whereas GFP-PMCA2wa was found only in the apical membrane, GFP-PMCA2za was present in both apical and basolateral membranes. The absence of immunochemical staining in the basolateral membrane with anti-PMCA2 antibodies reflects the very low abundance of the PMCA2za isoform, supporting our RT-PCR results. Alternatively, PMCA2za-detected mRNA could be either silenced in HCs or expressed by cochlear and vestibular ganglion neurons that are a potential contamination of the sensory epithelia preparation from which we extracted total mRNA.

A Leu-Ile motif in the b-tail is a basolateral signal for PMCA1 and PMCA2

The presence of the b-tail influences the trafficking of both PMCA1 and PMCA2. Deletion of the b-tail of PMCA1 leads to its targeting to both apical and basolateral membranes, replacement of the a-tail with the b-tail on PMCA2wa also results in its targeting to the apical and the basolateral membrane. One potential motif in the b-tail that could influence trafficking is the PDZ-binding domain at its C-terminus. PDZ interactions are known to influence the trafficking of many proteins (Cohen et al., 1998; Simske et al., 1996; Rongo et al., 1998). However, deletion of the last four aa of the b-tail of PMCA2xb did not alter its vectorial basolateral targeting. However, deletion of the entire b-tail of PMCA1xb, which is targeted exclusively to the basolateral membrane, resulted in targeting to both poles, showing that signal(s) in the b-tail play a role in basolateral targeting. Presumably, elimination of this signal results in a default mode

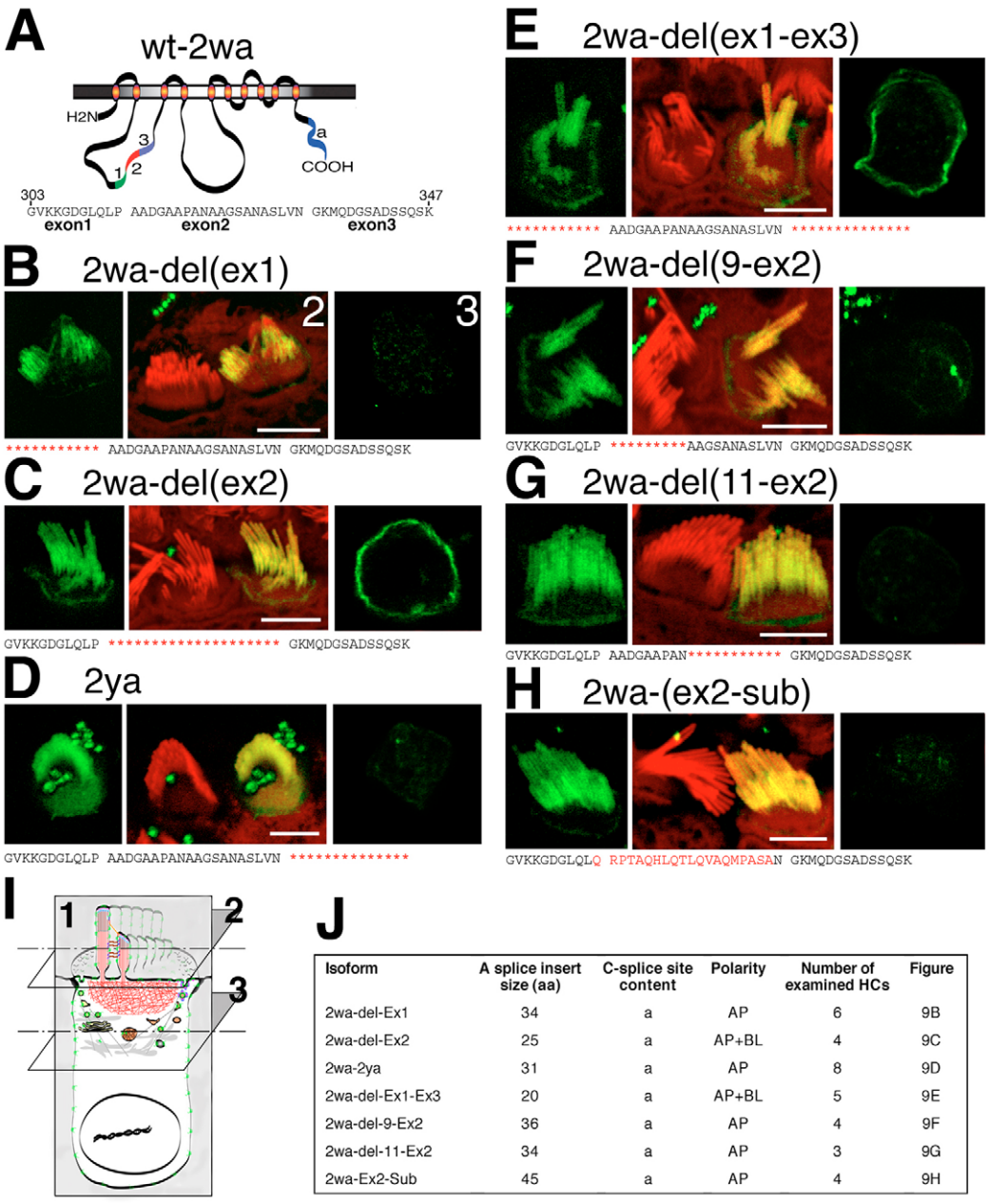

Isoform	A splice insert size (aa)	C-splice site content	Polarity	Number of examined HCs	Figure
2wa-del-Ex1	34	a	AP	6	9B
2wa-del-Ex2	25	a	AP+BL	4	9C
2wa-2ya	31	a	AP	8	9D
2wa-del-Ex1-Ex3	20	a	AP+BL	5	9E
2wa-del-9-Ex2	36	a	AP	4	9F
2wa-del-11-Ex2	34	a	AP	3	9G
2wa-Ex2-Sub	45	a	AP	4	9H

Fig. 9. The size of the insert of the A-splice site determines the apical targeting of PMCA2. (A) Schematic representation of the wild-type PMCA2wa isoform (wt-2wa) used to study the targeting properties of isoforms with various insert sizes. Aa sequence shows the three consecutive exons forming the w-insert of the A-splice site. (B-H) Confocal scans of the hair bundles (plane 2 in I; actin in red) of HCs expressing mutated variants of PMCA2wa (green) are shown in green and merged channels. High-resolution cross-sectional scans of the basolateral PM (plane 3 in I) are shown in the green channel. Mutations generated for each variant are shown in red on the aa sequence of the w-insert. (J) Summary of our results. Only isoforms with inserts of at least 31 aa in the A-splice site are targeted exclusively apically. a, a-tail; AP, apical PM localization; BL, basolateral PM localization. Bars, 5 μm.

of trafficking to both membranes. A second motif we investigated is a tyrosine motif (YEGL), a consensus binding-site for the μ subunits of AP adaptors (for a review, see Bonifacino and Traub, 2003). For the basolateral delivery, YxxΦ basolateral signals contained in PM proteins interact with adaptors of the clathrin type (AP1B) or non-clathrin type (AP4) at the trans Golgi network or the recycling endosomes. Mutation of this site did not influence basolateral trafficking. A third site that might influence trafficking is Leu1151 located downstream of an acidic cluster. The Leu-acidic cluster is homologous to the motif responsible for basolateral targeting of CD147 (Fig. 7) (Deora et al., 2004). This motif is functional in various epithelia including retinal pigment epithelia (RPE) of newborn rats (Marmorstein et al., 1996).

Through a deletion analysis, we identified a di-hydrophobic (Leu-Ile) motif that is conserved as a basolateral targeting motif in all rat and human PMCA1, PMCA 2 and PMCA3 b-splice variants. In PMCA4b, this di-hydrophobic motif is also well-conserved as Phe-Leu in rat, and as Leu-Leu sequence in human (see Fig. 7C). This di-hydrophobic motif has also been described as a basolateral targeting signal in many other proteins, including furin (for a review, see Bonifacino and Traub, 2003). The motif in PMCA is similar to the one identified for the basolateral targeting of E-cadherin (Fig. 7A) and conserved in many other members of the cadherin family (Miranda et al., 2001). Almost all known Leu-Leu-type motifs fit the consensus motifs (DE)xxxL(LI) and DxxLL (for a review, see Bonifacino and Traub, 2003). However, neither the sequences in the PMCAs, nor those in cadherins fit these consensus motifs. Leu-Leu motifs are generally found in an acidic context and are bordered by an acidic cluster, either N-terminally like in furin (Simmen et al., 1999), or C-terminally like in PMCAs and cadherins. In some cases, such as in furin, the acidic clusters (EEDE) located N-terminally to the Phe-Ile motif have been shown to be important for the function of the motif in basolateral targeting. However, we show that, in PMCA the acidic cluster located downstream of the dihydrophobic residues does not influence the basolateral targeting. One possible mechanism for the function of the Leu-Ile motif in basolateral trafficking involves Rab11 and the exocyst complex. Rab11 has been shown to regulate the basolateral delivery of wild-type *Drosophila* E-cadherin (dE-cadherin), which depends on a Leu-Leu motif (Lock and Stow, 2005). Rab11 and Armadillo interact with the exocyst components Sec15 and Sec10, respectively. Also, loss-of-function of Sec5, Sec6 and Sec15, components of the exocyst complex, results in the accumulation of dE-cadherin in a large, Rab11-recycling, endosomal compartment and inhibits the delivery of dE-cadherin to the PM (Langevin et al., 2005). These observations support a model whereby the exocyst regulates dE-Cadherin trafficking from recycling endosomes to sites on the epithelial cell membrane where Armadillo is located. A similar mechanism could regulate the trafficking of PMCA1 in HCs. A Leu-Leu motif has also been shown to regulate the trafficking of Shal K^+ channels to dendrites (Rivera et al., 2003).

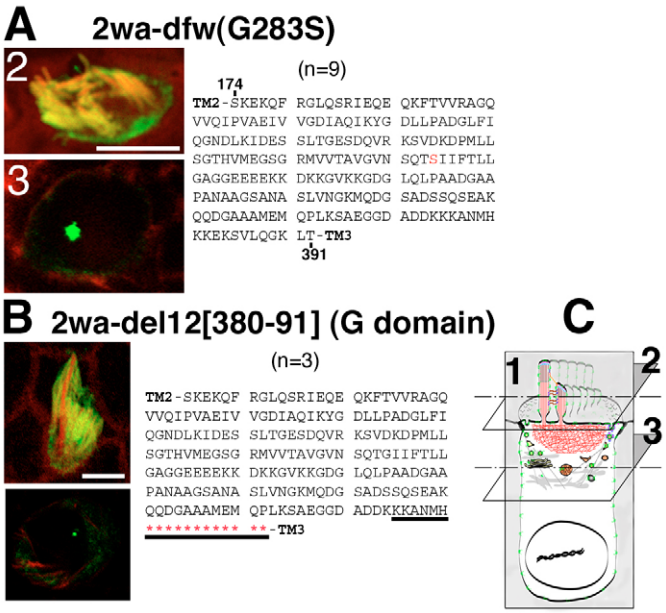

Fig. 10. PMCA2wa apical targeting is not altered by deafwaddler Gly283Ser mutation and is independent of its phospholipid activation site (G domain). (A,B) High-resolution confocal scans of the hair bundles (plane 2 in C, actin in red) and cross-sectional scans of the basolateral PM (plane 3 in C) of HCs expressing mutated variants of PMCA2wa (green) are shown in merged channels. (A) Deafwaddler mouse mutant (Dfw; Gly283Ser) and (B) del12[380-91] mutations are represented in red in the aa sequence of the second cytosolic loop of PMCA2wa, the phospholipids-binding site is underlined (B). Both mutated variants are targeted exclusively apically. TM, Transmembrane domain; n, number of examined transfected hair cells. Bars, 5 μm.

Apical targeting of PMCA2 depends on the alternatively spliced cassettes at the A-splice site

Targeting studies of GFP-constructs of the two PMCA2 isoforms PMCA2wa and PMCA2za detected in cochlea, suggested that the presence of the three alternatively spliced cassettes at the A-splice site plays a role in the apical targeting of PMCA2wa. PMCA2wa was targeted exclusively to the apical membrane whereas PMCA2za was delivered to both poles. Sequential deletion of the three alternatively spliced exons showed that PMCA2wa, PMCA2ya and PMCA2wa-del(ex-1) were all delivered exclusively to the apical membrane (Fig. 3A, Fig. 9D,B). However, larger deletions, such as in PMCA2wa-del(ex-2), PMCA2wa-del(ex1-ex3) and PMCA2za, were all delivered to both apical and basolateral membranes, suggesting that the size of the insert influenced the trafficking. This was confirmed by substituting an unrelated aa sequence with exon 2, in which case the product was – like PMCA2wa, which has the same-sized insert of 45 amino acids – delivered exclusively to the apical membrane.

The maximum number of aa for PMCA1, PMCA3 and PMCA4 A-splice-site cassettes is 13, 14 and 12 aa, respectively (for a review, see Strehler and Zacharias, 2001). We showed that in PMCA2, A-splice inserts of 31 aa or more are required to target the protein exclusively to the apical membrane (Fig. 9). Therefore, whatever the A-splice-site variant is, the b-tail containing isoforms of PMCA3 and (human) PMCA4 should be targeted exclusively basolaterally, as do PMCA1xb and PMCA2zb and PMCA2xb (Fig. 4B, Fig. 3E, Fig. 6B). The nature of the PMCA3 isoform, expressed in rat vestibular HCs

and immunolocalized basolaterally (Dumont et al., 2001), has not been reported. RT-PCR data combined with our targeting results, showing the requirement of the b-tail for basolateral targeting, suggest that PMCA3b is the major splice form expressed in HCs (our unpublished observation).

Our finding that the size of the A-splice site, but not its composition, is important for apical targeting suggests that a particular motif, which controls targeting, is not present in the alternatively spliced cassettes. Rather, these results suggest that the size of the insert alters the conformation of the cytoplasmic loop and may affect the availability of motifs elsewhere in the loop. We investigated two possible sites in the loop for their implication in the apical targeting of PMCA2, the mutation site that causes deafness in the deafwaddler mouse and the phospholipid-binding domain. Mutation of either of these sites did not alter trafficking of PMCA2. Further investigations on PMCA2 apical targeting elements would include the remaining sequences in the loop as well as the bordering TMs.

Materials and Methods

Whole mount preparation of adult rat organs of Corti

Three-week to 6-week-old rats were anesthetized with CO_2 and decapitated according to National Institutes of Health (NIH) guidelines. Cochleae were freshly dissected and fixed with 4% paraformaldehyde (PFA), injected into the membranous labyrinth through the round and oval windows and incubated for 30 minutes at room temperature. After removing the bone, the tectorial membrane was removed and organ of Corti pieces were isolated from different turns of the cochlea and processed for immunofluorescence.

Cloning of rat organ of Corti PMCA2 isoforms and cDNA constructs

Full-length cDNAs encoding PMCA2 isoforms PMCA2wa (1199 aa) and PMCA2za (1154 aa) expressed in rat inner ear sensory epithelia were obtained from total mRNA prepared from P2 to P15 rat vestibular neuroepithelia and organ of Corti sensory patches by using Triazol (Life Technologies, MD). Gene-specific reverse transcription (RT) was performed on DNase-treated mRNA with the primer 5′-GGGCCTCAGCTAAAGCG-3′ and MuMLV reverse transcriptase (GibcoBRL, CA), followed by a PCR reaction with the forward primer: 5′-atgtgaagcttg-GGTGATATGACCAACAGCGACTTTTAC-3′ and the reverse primer: 5′-gcaaggtacc-GCTAAAGCGACGTCTCCAGGCTGTGG-3′ using High-Fidelity Taq Polymerase (Invitrogen, CA) (lowercase sequences correspond to inserted flanking *Hin*dIII and *Kpn*I restriction sites used for directional cloning in pEGFP-C2). The RT-PCR products were cloned into the pCR2.1 TA cloning vector (Invitrogen, CA), and their A-splice region and their 3′-termini sequences were sequenced to identify the PMCA2wa and PMCA2za isoforms.

To characterize the splicing events that occur in rat cochlea and vestibular hair cells, we randomly reverse-transcribed 5 μg of RNase-free DNase-I-treated total mRNA and PCR-amplified the cDNA regions encoding for the C-terminal tails with primers C-PMCA2-F 5′-CCGGGGCCTGAATCGGATCC-3′ and C-PMCA2-R 5′-GGATGGGGCTCCCTGGACTTG-3′ or C-PMCA1-F 5′-GATGTTGAAGA-GATTGACCATGCCG and C-PMCA1-R 5′-CTTACAATCAGAGTGATGTTT-CCAAACTATG, and part of the second intracellular loop, including the A-splice-site cDNA sequence with primers A-PMCA2-F 5′-GAAAGCTCGCTCACAGGG-GAG-3′ and A-PMCA2-R 5′-ACCCATGGTCTCACAGGCG-3′ or A-PMCA1-F 5′-GACGAGAGTTCGTTGACTGGCGAG and A-PMCA1-R: GATTGGCGTG-CACTCAGCAAGCCACGG. After 25 cycles of amplification of the PMCA1 and PMCA2 C-splice-site regions, and PMCA1 A-splice-site region, samples of the RT-PCR product were loaded on a 2%-agarose gel containing ethidium bromide. For cDNA amplicons of the PMCA2 A-splice-site region, 4 μl of each sample was tested after 15, 18, 21 and 25 cycles of amplification, and emitted fluorescence under UV-light excitation was collected on digital images (NIH). cDNA amplicons were randomly cloned into the pCR2.1 TA cloning vector (Invitrogen, CA), and more than a hundred clones for each RT-PCR product were sequenced for their content using an ABI-3100 Avant (Applied Biosystems, CA).

The full-length human PMCA1xb coding sequence was assembled from PCR fragments following a strategy described earlier, and cloned into the expression vector pMM2 (Adamo et al., 1992). The entire cDNA coding from residue Gly2 to the C-terminal residue Leu1220 was amplified from this construct with primers SacI-hPMCA1-F 5′-ggcggcgcggagctcGGGCGACATGGCAAACAACTCAG and KpnI-hPMCA1-R 5′-ggccggtaccTCAGAGTGATGTTTCC, and directionally cloned into the pEGFP-C2 vector (Clontech, CA). Sequencing of the full-length cDNA revealed two aa substitutions in the first cytoplasmic loop of the encoded proteins (M267R and N281R) and two aa substitutions in the second cytoplasmic loop (V588I and K747R) (supplementary material Fig. S1). The imaged HCs (Fig. 4), which expressed EGFP-tagged PMCA1xb and PMCA1xb-del b were transfected with constructs encoding proteins containing the substitutions. The reversion of both substitutions in the first cytoplasmic loop did not change the targeting properties of the encoded proteins (data not shown). EGFP-tagged PMCA2wa and PMCA2za were generated by directional cloning of inserts from clones described above into *Hin*dIII and *Kpn*I cloning sites of the pEGFP-C2 vector (Clontech, CA). The construct encoding EGFP-tagged human PMCA2xb (1212 aa) has been previously described (Chicka and Strehler, 2003). Chimeric fusions between cDNAs encoding either the a or b C-terminal splice variants (59aa or 103 aa, respectively) and the cDNA encoding for TAC were generated in a pCDNA3 expression vector (Invitrogen, CA) using standard PCR methods. A QuickChange site-directed mutagenesis kit (Stratagene, CA) was used to introduce stop codons, deletions, and substitutions in the EGFP-tagged PMCA1xb, PMCA2xb, PMCA2za and PMCA2wa, as well as TAC chimera. All constructs were verified by DNA sequencing.

Organotypic cultures of organ of Corti and vestibular sensory patches from rat, and ballistic transfection of hair cells

Organotypic cultures of organ of Corti and vestibular sensory epithelia from rat were prepared according to Sobkowicz et al. (Sobkowicz et al., 1993), and modified as described by Rzadzinska et al. (Rzadzinska et al., 2004). Postnatal day 0-4 rat pups were anesthetized with CO_2 and decapitated according to NIH guidelines; their temporal bones were isolated and placed into Leibovitz L-15 media (GIBCO, CA). The dissected organ of Corti was split into two to four pieces for culturing, and the otoconia were removed from above the vestibular sensory epithelia. Tissues were attached to dishes with coverslips in the bottom that had been coated with CellTak (BD Biosciences, MD) and placed in culture dishes (MatTek, MA). Cultures were incubated at 37°C and 5% CO_2 in DMEM F-12 media supplemented with 5% fetal bovine serum (FBS) containing 10 μg/ml ampicillin (GIBCO, CA). Explants were maintained in culture for 1-7 days. The inner ear explants were transfected with 1 μm gold particles coated with plasmid DNA, by using a Helios Gene Gun (Bio-Rad Laboratories, CA). Explants were fixed with 4% paraformaldehyde (PFA) in PBS 24 hours after transfection, permeabilized with 0.5% Triton X-100 in PBS and counterstained for actin with Rhodamine-coupled phalloidin for 30 minutes. The specimens were finally mounted with Antifade Mounting medium (Molecular Probes, CA).

Cell culture and transient transfections of MDCK-I and LLC-PK1 cells

LLC-PK1 (CL-101) and MDCKI (NBL-2; CCL-34) cells were obtained from American Type Culture Collection (ATCC; VA). We used a standard transfection technique with Lipofectamine-2000 as described by the manufacturer (Invitrogen, CA). Briefly, MDCK cells were grown on glass coverslips and LLC-PK1 were polarized on 0.4 μm TransWells in DMEM medium (Life Technologies, MD) supplemented with 10% serum. Cells were washed with serum-free DMEM 3 hours before transfection. DNA-Lipofectamine complex prepared in serum-free medium was added to the apical side. Cells were incubated with DNA-Lipofectamine for 6 hours at 37°C, 5% CO_2. After 6 hours, the medium was replaced by regular DMEM serum-containing medium. Monolayers were analyzed 24 hours after transfection by immunofluorescence.

Immunofluorescence and confocal microscopy

The following primary antibodies were used: rat anti-ZO-1 (1:300 dilution; Chemicon, CA), rabbit anti-PMCA2 (1:300 dilution; SWANT, Switzerland), rabbit anti PMCA1 (1:300 dilution; Abcam, MA), mouse anti-TAC (ATCC, VA), secondary Alexa Fluor-555 goat anti-rat, Alexa Fluor-468 rat anti-goat, or Alexa Fluor-468 goat anti-mouse (Molecular Probes, CA). Cell monolayers and cochlear cultures were fixed for 20 minutes with 4% PFA prepared in PBS and quenched with 50 mM NH_4Cl in PBS (containing 1 mM $CaCl_2$ and 1 m $MMgCl_2$). Cells were then permeabilized with 0.5% Triton X-100 for 15 minutes and blocked with 10% FBS/PBS for 30 minutes. Primary antibodies were applied for 1 hour at room temperature. The specimens were washed three times for 15 minutes with PBS and incubated with fluorescent secondary antibodies. High-resolution confocal images (2048×2048 pixels) were taken at room temperature with an LSM510 Zeiss microscope with a 63× NA=1 oil objective (Carl Zeiss, NY). 3D-images were built from stacks of serial (0.8 μm) *x-y* (en face) confocal images (512×512 pixels) using Volocity software (Improvision, MA).

We thank L. A. Dunbar and R. S. Petralia (NIDCD/NIH) for their helpful discussions while assembling and writing the manuscript, and B. Kachar (NIDCD/NIH) and R. Weigert (NHLBI/NIH) for their critical reading of the manuscript. This work was supported by the Intramural Research Program of NIDCD. E.E.S. was supported by grant GM28835 from the NIH.

References

Adamo, H. P., Verma, A. K., Sanders, M. A., Heim, R., Salisbury, J. L., Wieben, E. D. and Penniston, J. T. (1992). Overexpression of the erythrocyte plasma membrane Ca2+ pump in COS-1 cells. *Biochem. J.* **285**, 791-797.

Aroeti, B., Kosen, P. A., Kuntz, I. D., Cohen, F. E. and Mostov, K. E. (1993). Mutational and secondary structural analysis of the basolateral sorting signal of the polymeric immunoglobulin receptor. *J. Cell Biol.* **123**, 1149-1160.

Bonifacino, J. S. and Dell'Angelica, E. C. (1999). Molecular bases for the recognition of tyrosine-based sorting signals. *J. Cell Biol.* **145**, 923-926.

Bonifacino, J. S. and Traub, L. M. (2003). Signals for sorting of transmembrane proteins to endosomes and lysosomes. *Annu. Rev. Biochem.* **72**, 395-447.

Chicka, M. C. and Strehler, E. E. (2003). Alternative splicing of the first intracellular loop of plasma membrane Ca^{2+}-ATPase isoform 2 alters its membrane targeting. *J. Biol. Chem.* **278**, 18464-18470.

Chuang, J. Z. and Sung, C. H. (1998). The cytoplasmic tail of rhodopsin acts as a novel apical sorting signal in polarized MDCK cells. *J. Cell Biol.* **142**, 1245-1256.

Cohen, A. R., Woods, D. F., Marfatia, S. M., Walther, Z., Chishti, A. H. and Anderson, J. M. (1998). Human CASK/LIN-2 binds syndecan-2 and protein 4.1 and localizes to the basolateral membrane of epithelial cells. *J. Cell Biol.* **142**, 129-138.

Deora, A. A., Gravotta, D., Kreitzer, G., Hu, J., Bok, D. and Rodriguez-Boulan, E. (2004). The basolateral targeting signal of CD147 (EMMPRIN) consists of a single leucine and is not recognized by retinal pigment epithelium. *Mol. Biol. Cell* **15**, 4148-4165.

Dumont, R. A., Lins, U., Filoteo, A. G., Penniston, J. T., Kachar, B. and Gillespie, P. G. (2001). Plasma membrane Ca^{2+}-ATPase isoform 2a is the PMCA of hair bundles. *J. Neurosci.* **21**, 5066-5078.

Filoteo, A. G., Enyedi, A. and Penniston, J. T. (1992). The lipid-binding peptide from the plasma membrane Ca^{2+} pump binds calmodulin, and the primary calmodulin-binding domain interacts with lipid. *J. Biol. Chem.* **267**, 11800-11805.

Folsch, H., Ohno, H., Bonifacino, J. S. and Mellman, I. (1999). A novel clathrin adaptor complex mediates basolateral targeting in polarized epithelial cells. *Cell* **99**, 189-198.

Gan, Y., McGraw, T. E. and Rodriguez-Boulan, E. (2002). The epithelial-specific adaptor AP1B mediates post-endocytic recycling to the basolateral membrane. *Nat. Cell Biol.* **4**, 605-609.

Guerini, D., Coletto, L. and Carafoli, E. (2005). Exporting calcium from cells. *Cell Calcium* **38**, 281-289.

Hunziker, W. and Fumey, C. (1994). A di-leucine motif mediates endocytosis and basolateral sorting of macrophage IgG Fc receptors in MDCK cells. *EMBO J.* **13**, 2963-2969.

Ikonen, E. (2001). Roles of lipid rafts in membrane transport. *Curr. Opin. Cell Biol.* **13**, 470-477.

Jacob, R., Alfalah, M., Grunberg, J., Obendorf, M. and Naim, H. Y. (2000). Structural determinants required for apical sorting of an intestinal brush-border membrane protein. *J. Biol. Chem.* **275**, 6566-6572.

Janvier, K., Kato, Y., Boehm, M., Rose, J. R., Martina, J. A., Kim, B. Y., Venkatesan, S. and Bonifacino, J. S. (2003). Recognition of dileucine-based sorting signals from HIV-1 Nef and LIMP-II by the AP-1 gamma-sigma1 and AP-3 delta-sigma3 hemicomplexes. *J. Cell Biol.* **163**, 1281-1290.

Kalinec, F., Holley, M. C., Iwasa, K. H., Lim, D. J. and Kachar, B. (1992). A membrane-based force generation mechanism in auditory sensory cells. *Proc. Natl. Acad. Sci. USA* **89**, 8671-8675.

Keller, P. and Simons, K. (1997). Post-Golgi biosynthetic trafficking. *J. Cell Sci.* **110**, 3001-3009.

Klapper, M., Daniel, H. and Doering, F. (2006). The cytosolic C-terminus of the peptide transporter PEPT2 is involved in apical membrane localization of the protein. *Am. J. Physiol. Cell Physiol.* **290**, C472-C483.

Kundu, A., Avalos, R. T., Sanderson, C. M. and Nayak, D. P. (1996). Transmembrane domain of influenza virus neuraminidase, a type II protein, possesses an apical sorting signal in polarized MDCK cells. *J. Virol.* **70**, 6508-6515.

Langevin, J., Morgan, M. J., Sibarita, J. B., Aresta, S., Murthy, M., Schwarz, T., Camonis, J. and Bellaiche, Y. (2005). Drosophila exocyst components Sec5, Sec6, and Sec15 regulate DE-Cadherin trafficking from recycling endosomes to the plasma membrane. *Dev. Cell* **9**, 355-376.

Le Gall, A. H., Yeaman, C., Muesch, A. and Rodriguez-Boulan, E. (1995). Epithelial cell polarity: new perspectives. *Semin. Nephrol.* **15**, 272-284.

Lin, S., Naim, H. Y., Rodriguez, A. C. and Roth, M. G. (1998). Mutations in the middle of the transmembrane domain reverse the polarity of transport of the influenza virus hemagglutinin in MDCK epithelial cells. *J. Cell Biol.* **142**, 51-57.

Lisanti, M. P., Caras, I. W., Davitz, M. A. and Rodriguez-Boulan, E. (1989). A glycophospholipid membrane anchor acts as an apical targeting signal in polarized epithelial cells. *J. Cell Biol.* **109**, 2145-2156.

Lock, J. G. and Stow, J. L. (2005). Rab11 in recycling endosomes regulates the sorting and basolateral transport of E-cadherin. *Mol. Biol. Cell* **16**, 1744-1755.

Marmorstein, A. D., Bonilha, V. L., Chiflet, S., Neill, J. M. and Rodriguez-Boulan, E. (1996). The polarity of the plasma membrane protein RET-PE2 in retinal pigment epithelium is developmentally regulated. *J. Cell Sci.* **109**, 3025-3034.

Matter, K., Hunziker, W. and Mellman, I. (1992). Basolateral sorting of LDL receptor in MDCK cells: the cytoplasmic domain contains two tyrosine-dependent targeting determinants. *Cell* **71**, 741-753.

Miranda, K. C., Khromykh, T., Christy, P., Le, T. L., Gottardi, C. J., Yap, A. S., Stow, J. L. and Teasdale, R. D. (2001). A dileucine motif targets E-cadherin to the basolateral cell surface in Madin-Darby canine kidney and LLC-PK1 epithelial cells. *J. Biol. Chem.* **276**, 22565-22572.

Mostov, K. E., Verges, M. and Altschuler, Y. (2000). Membrane traffic in polarized epithelial cells. *Curr. Opin. Cell Biol.* **12**, 483-490.

Nelson, W. J. and Yeaman, C. (2001). Protein trafficking in the exocytic pathway of polarized epithelial cells. *Trends Cell Biol.* **11**, 483-486.

Ohno, H., Aguilar, R. C., Yeh, D., Taura, D., Saito, T. and Bonifacino, J. S. (1998). The medium subunits of adaptor complexes recognize distinct but overlapping sets of tyrosine-based sorting signals. *J. Biol. Chem.* **273**, 25915-25921.

Ohno, H., Tomemori, T., Nakatsu, F., Okazaki, Y., Aguilar, R. C., Foelsch, H., Mellman, I., Saito, T., Shirasawa, T. and Bonifacino, J. S. (1999). Mu1B, a novel adaptor medium chain expressed in polarized epithelial cells. *FEBS Lett.* **449**, 215-220.

Qi, A. D., Wolff, S. C. and Nicholas, R. A. (2005). The apical targeting signal of the P2Y2 receptor is located in its first extracellular loop. *J. Biol. Chem.* **280**, 29169-29175.

Rapoport, I., Chen, Y. C., Cupers, P., Shoelson, S. E. and Kirchhausen, T. (1998). Dileucine-based sorting signals bind to the beta chain of AP-1 at a site distinct and regulated differently from the tyrosine-based motif-binding site. *EMBO J.* **17**, 2148-2155.

Rivera, J. F., Ahmad, S., Quick, M. W., Liman, E. R. and Arnold, D. B. (2003). An evolutionarily conserved dileucine motif in Shal K+ channels mediates dendritic targeting. *Nat. Neurosci.* **6**, 243-250.

Rodionov, D. G., Nordeng, T. W., Kongsvik, T. L. and Bakke, O. (2000). The cytoplasmic tail of CD1d contains two overlapping basolateral sorting signals. *J. Biol. Chem.* **275**, 8279-8282.

Rodriguez-Boulan, E. and Gonzalez, A. (1999). Glycans in post-Golgi apical targeting: sorting signals or structural props? *Trends Cell Biol.* **9**, 291-294.

Rongo, C., Whitfield, C. W., Rodal, A., Kim, S. K. and Kaplan, J. M. (1998). LIN-10 is a shared component of the polarized protein localization pathways in neurons and epithelia. *Cell* **94**, 751-759.

Roush, D. L., Gottardi, C. J., Naim, H. Y., Roth, M. G. and Caplan, M. J. (1998). Tyrosine-based membrane protein sorting signals are differentially interpreted by polarized Madin-Darby canine kidney and LLC-PK1 epithelial cells. *J. Biol. Chem.* **273**, 26862-26869.

Rzadzinska, A. K., Schneider, M. E., Davies, C., Riordan, G. P. and Kachar, B. (2004). An actin molecular treadmill and myosins maintain stereocilia functional architecture and self-renewal. *J. Cell Biol.* **164**, 887-897.

Scheiffele, P., Peranen, J. and Simons, K. (1995). N-glycans as apical sorting signals in epithelial cells. *Nature* **378**, 96-98.

Schultz, J. M., Yang, Y., Caride, A. J., Filoteo, A. G., Penheiter, A. R., Lagziel, A., Morell, R. J., Mohiddin, S. A., Fananapazir, L., Madeo, A. C. et al. (2005). Modification of human hearing loss by plasma-membrane calcium pump PMCA2. *N. Engl. J. Med.* **352**, 1557-1564.

Simmen, T., Nobile, M., Bonifacino, J. S. and Hunziker, W. (1999). Basolateral sorting of furin in MDCK cells requires a phenylalanine-isoleucine motif together with an acidic amino acid cluster. *Mol. Cell. Biol.* **19**, 3136-3144.

Simonsen, A., Stang, E., Bremnes, B., Roe, M., Prydz, K. and Bakke, O. (1997). Sorting of MHC class II molecules and the associated invariant chain (Ii) in polarized MDCK cells. *J. Cell Sci.* **110**, 597-609.

Simske, J. S., Kaech, S. M., Harp, S. A. and Kim, S. K. (1996). LET-23 receptor localization by the cell junction protein LIN-7 during C. elegans vulval induction. *Cell* **85**, 195-204.

Sobkowicz, H. M., Loftus, J. M. and Slapnick, S. M. (1993). Tissue culture of the organ of Corti. *Acta Otolaryngol.* **502**, 3-36.

Street, V. A., McKee-Johnson, J. W., Fonseca, R. C., Tempel, B. L. and Noben-Trauth, K. (1998). Mutations in a plasma membrane Ca^{2+}-ATPase gene cause deafness in deafwaddler mice. *Nat. Genet.* **19**, 390-394.

Strehler, E. E. and Zacharias, D. A. (2001). Role of alternative splicing in generating isoform diversity among plasma membrane calcium pumps. *Physiol. Rev.* **81**, 21-50.

Wan, L., Molloy, S. S., Thomas, L., Liu, G., Xiang, Y., Rybak, S. L. and Thomas, G. (1998). PACS-1 defines a novel gene family of cytosolic sorting proteins required for trans-Golgi network localization. *Cell* **94**, 205-216.

Wood, J. D., Muchinsky, S. J., Filoteo, A. G., Penniston, J. T. and Tempel, B. L. (2004). Low endolymph calcium concentrations in deafwaddler2J mice suggest that PMCA2 contributes to endolymph calcium maintenance. *J. Assoc. Res. Otolaryngol.* **5**, 99-110.

Yamoah, E. N., Lumpkin, E. A., Dumont, R. A., Smith, P. J., Hudspeth, A. J. and Gillespie, P. G. (1998). Plasma membrane Ca^{2+}-ATPase extrudes Ca^{2+} from hair cell stereocilia. *J. Neurosci.* **18**, 610-624.

Yeaman, C., Le Gall, A. H., Baldwin, A. N., Monlauzeur, L., Le Bivic, A. and Rodriguez-Boulan, E. (1997). The O-glycosylated stalk domain is required for apical sorting of neurotrophin receptors in polarized MDCK cells. *J. Cell Biol.* **139**, 929-940.

Yeaman, C., Grindstaff, K. K. and Nelson, W. J. (1999). New perspectives on mechanisms involved in generating epithelial cell polarity. *Physiol. Rev.* **79**, 73-98.